



## OFFICE MEMORANDUM

TO : Distribution

DATE: April 24, 1981

FROM : H. N. Fisher

SUBJECT : DEVELOPMENT OF THE PHASE I HDR RESERVOIR: PART II, GENERAL CHARACTERISTICS

SYMBOL : G-6

MAIL STOP: 981

### INTRODUCTION

In Part I of this memo the growth of the Phase I reservoir was traced in terms of changes in the following parameters:

- o Heat exchange areas
- o Tracer volumes
- o Number of fractures
- o Average fracture apertures
- o Average fracture widths.

This was done for the total system and in some cases for individual flow paths.

Here, the following topics are reviewed:

- o The relation of the long-term water loss to reservoir size and heat exchange area.
- o The relation of the loci of microseismic events to reservoir size and heat exchange area.
- o The recent (81/03/17) post Expt. 217 temperature log in EE-1 and the possibility of reservoir growth during Expt. 217.

### II. LONG-TERM WATER LOSS FOR EXPT. 217

The data for the water loss during Expt. 217 and the status of the analysis is discussed in Appendix C.

The water loss is only 30 percent higher than that of Segment 2. The heat exchange area was a factor of 2.5 to 5 larger during Expt. 217 than during Segment 2 (see Part I of this memo). Also estimates of a diffusion area associated with the water losses indicate a limiting area many times the heat exchange area (Ref. 4). An obvious conclusion is that the heat exchange system utilizes a small portion of a much larger fracture system that controls water loss. This large fracture system was

not altered to any large extent by the MHF experiments of Segment 4. The heat exchange area has changed rapidly compared to any area associated with the water loss.

### III. LOCI OF MICROSEISMIC EVENTS

The loci of the microseismicity has always occupied a volume of rock large compared to any possible volume of the cooled reservoir (Ref. 3 and 5). This large volume is part of the pressurized storage volume associated with short- and long-term water loss. Most of the seismic experiments (Segments 4 and SUE) are for pressure increases of one day or less duration. The large extent of the loci indicate that fractures of intermediate size and permeability are being pressurized and not the small-scale porosity. Here one example from Segment 4 will be examined. Figure 1 is a projection of the accumulated microseismic events on the horizontal plane (Ref. 3 and 5). The main group of points occupies an area 400 meters by ~100 meters. This same accumulation of events has a vertical extent of 300 meters and hence, a vertical projected area of  $400 \times 300 = 120,000 \text{ m}^2$ . However, since there is considerable evidence for multiple fracture (Part I), it is reasonable to interpret this microseismicity as occurring in or near the extensions of the fractures that form the heat exchange system. If three fractures are involved the total area is  $360,000 \text{ m}^2$ . It is likely that the actual fracture system is fairly complicated containing many fractures and cross joints.

### IV. POST EXPERIMENT 217 TEMPERATURE LOGS IN EE-1

Two post Expt. 217 temperature logs are now available for EE-1. In Fig. 2 they are compared with the last log before Expt. 217. Each major temperature depression is labeled with the flow segment that produced the major part of it. This data must be subject to a detail computer analysis in terms of specific models. For now we examine three significant general features of the logs.

The most recent log (81/01/21 (2) of Fig. 2) is beginning to show considerable structure. In addition to the flow entrance at A in the figure, there are three distinct fracture intersections with the wellbore located at B, C, and D in the lower half of the wellbore. Since two of these may represent the same fracture crossing the curved wellbore twice, there are at least two fractures sharing the inlet flow.

The local maximum in the temperature located at E in the figure was due to the presence of an undepleted portion of the reservoir. As the cooling wave moves up through the reservoir this maximum first moves up (curves (1) and (2)) then during recovery moves back down. The highest vertical excursion of this maximum indicates that the cooling wave is not moving through the reservoir as fast as previous (Part I and Ref. 6) analyses have indicated. This maximum has not reached the vertical position of the flow exits in GT-2B located at L, M, and U in the figure.

The vertical extent of the depleted region for Segment 5 is also somewhat less than that indicated by an extrapolation from the Segment 4. The depletion is confined to the lower half of the reservoir. The flow duration for Segment 4 was thirteen times longer than that of Segment 5 and the average flow rate was somewhat higher. Scaling with the square root of the flow duration and directly with flow rate would indicate that the width of the Segment 5 temperature depression should be over 200 meters wide rather than the 150 meters indicated by the figure.

Any interpretation of these observations must be qualified by the fact that the reservoir is heterogeneous and contains several fractures. However some questions can be raised and tentative conclusions reached.

- o The lower portion of the reservoir may contain three or more fractures.
- o The curvature observed in the Expt. 217 outlet temperature curves may not be drawdown, but may be due mostly to the Segment 2, 3 temperature depression reaching the outlets.
- o The total fracture width in the lower portion of the reservoir is larger than that observed in Expt. 215.

The Expt. 217 outlet temperatures and the EE-1 temperature logs need to be examined in terms of specific heat conduction models.

#### V. SUMMARY

A number of important general reservoir characteristics can now be listed.

1) Pressurization and cooling have resulted in the development of complex multi-fracture systems associated with all pressurized wellbore segments with the possible exception of the original GT-2. Figures 3 and 4 located the major flow entrances and fracture crossings  $\oplus$  as observed in the temperature logs. These represent only those fractures with

significant cooling and do not reflect the multiplicity of joints identifiable by tracer studies.

2) The heat exchange area is small compared to areas identified by other methods. Table 1 lists some of these area estimates. The extremely large inflation areas are obtained from total injected volumes divided by a nominal 1 mm aperture. The actual area associated with this volume could be larger as some of the water must be in small scale porosity with smaller apertures. Most of this area cannot be expected to participate in heat exchange flow.

The seismic area is the vertical projection of the locus of seismicity (section III) multiplied by N, the number of fractures in the microseismic volume. For N=3 the areas are very close to the diffusion area. The diffusion area is obtained mainly from water loss data. The assumptions used to obtain this area are discussed in ref. 4.

An area can be obtained from the volume of water vented at high flow rates after the system has been pressurized for a long time. The higher vent rates are assumed to come from a large low impedance system before the decreasing internal pressure closes the fractures. The vent areas in the table are for a fracture system with a 4 mm aperture at the start of the vents. This 4 mm aperture is consistent with the values obtained for the pressurized flow through system in Ref. 4 and Part I of this memo.

The heat exchange areas as determined in Part I of this memo are in the final columns of the table and are seen to be small compared to any other area estimate. This indicates that only a small portion of the pressurized fracture system is being utilized as heat exchange area.

3) The heat exchange area grows during drawdown and the additional area is in the partially depleted portions of the reservoir. Changes of reservoir geometry have produced modest new hot heat exchange area. Repressurization has increased the heat exchange area in the depleted portions of the reservoir. Figure 5 traces the growth of the heat exchange area and the modal tracer volumes throughout Phase I. The area increases are from the analysis are from Part I and the volumes from Refs. 3 and 6.

The initial area of 7500 m<sup>2</sup> was established by many pressurizations and some cooling. This area grew to 15,000 m<sup>2</sup> in the 75 day drawdown of Segment 2. The high back pressure of Segment 3 (Ref. 2) caused a

redistribution of flow and the heat exchange area started at 6,000 m<sup>2</sup> and grew to 12,000 m<sup>2</sup> during the 28 day flow. The temperature history and flow geometry indicate that this was the same area involved in Segment 2.

The system was pressurized to high pressures several times during Segment 4 but no area or volume measurements made until Expt. 215. After 215 the EE-1 temperature logs indicated that between 6000 and 9000 m<sup>2</sup> had been added to the lower part of the reservoir by the recementing and pressurization of Segment 4. This increased the measured heat exchange area to between 21,000 and 24,000 m<sup>2</sup>.

The area measurements during Segment 5 are somewhat uncertain (Part I and section IV). The best estimates are that the heat exchange area was at least 37,000 m<sup>2</sup> at the start of flow and at least 45,000 m<sup>2</sup> at the end. The lack of recovery of the outlet temperature indicates that the additional area is in the depleted upper half of the reservoir or was partly added to the lower half as Expt. 217 proceeded.

#### REFERENCES

1. J. W. Tester and J. N. Albright (eds.), "Hot Dry Rock Energy Extraction Field Test: 75 Days of Operation of a Prototype Reservoir at Fenton Hill," Los Alamos National Laboratory report LA-7771-MS (April 1979).
2. D. W. Brown, "Results of Expt. 186, The High Back-Pressure Flow Experiment," (in preparation).
3. HDR Staff, "Preliminary Evaluation of the Second Hot Dry Rock Geothermal Energy Reservoir: Results of Phase I, Run Segment 4," Los Alamos National Laboratory report LA-8354-MS (May 1980).
4. H. N. Fisher and J. W. Tester, "The Pressure Transient Testing of a Man-Made Fractured Geothermal Reservoir: An Examination of Fracture Versus Matrix Dominated Flow Effect," LA-8535-MS (Sept. 1980).
5. HDR Staff, "Preliminary Report on Stress Unlocking Experiment (SUE)," Los Alamos National Laboratory Memorandum, Feb. 29, 1981.
6. HDR Staff, "Preliminary Report on Segment V," in preparation.

Distribution:

R. R. Brownlee, G-DO  
G. Nunz, EP/AES  
J. Rowley, G-2  
B. Killian, G-DO  
M. C. Smith, G-DOF  
R. Spence, G-DOT  
C. Keller, G-6  
J. Hill, G-2  
L. Aamodt, G-5  
R. Hendron, G-2  
D. Brown, G-5  
R. Potter, G-5  
H. Murphy, G-5  
G. Zyvoloski, G-5  
F. Walter, G-5  
H. Keppler, G-5  
B. Hoffers, G-5  
H. Fisher, G-6  
J. Tester, MIT  
G-5 file

TABLE 1.

AREA (m<sup>2</sup>)

SEGMENT	INFLATION*	SEISMIC	DIFFUSION**	VENT	HEAT TRANSFER
1		>20 000			
2	5 x 10 <sup>6</sup>		~250 000	40 000	7 500 15 000
3	5 x 10 <sup>6</sup>				6 000 12 000
4		120,000 x N			>21 000
5	20 x 10 <sup>6</sup>	~120,000 x N	~350 000	>250 000 <sup>†</sup>	37 000 45 000

\*1 MM APERTURE

\*\*k = 10<sup>-19</sup> m<sup>2</sup>, C = 4.0 x 10<sup>-5</sup> MPa<sup>-1</sup>

†4 mm APERTURE

FIG. 1 LOCUS OF MICROSEISMICITY - SEG. 4.

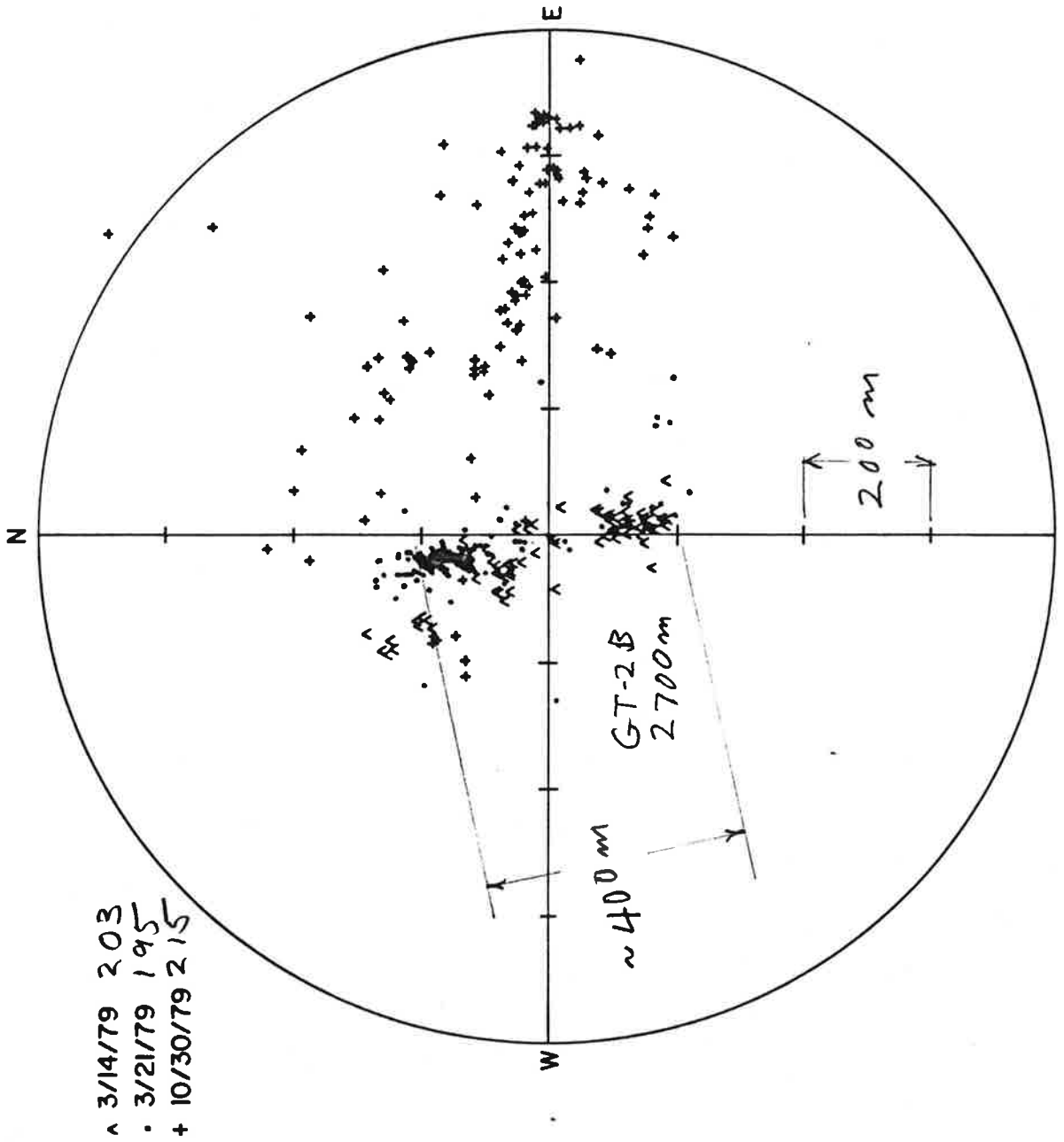
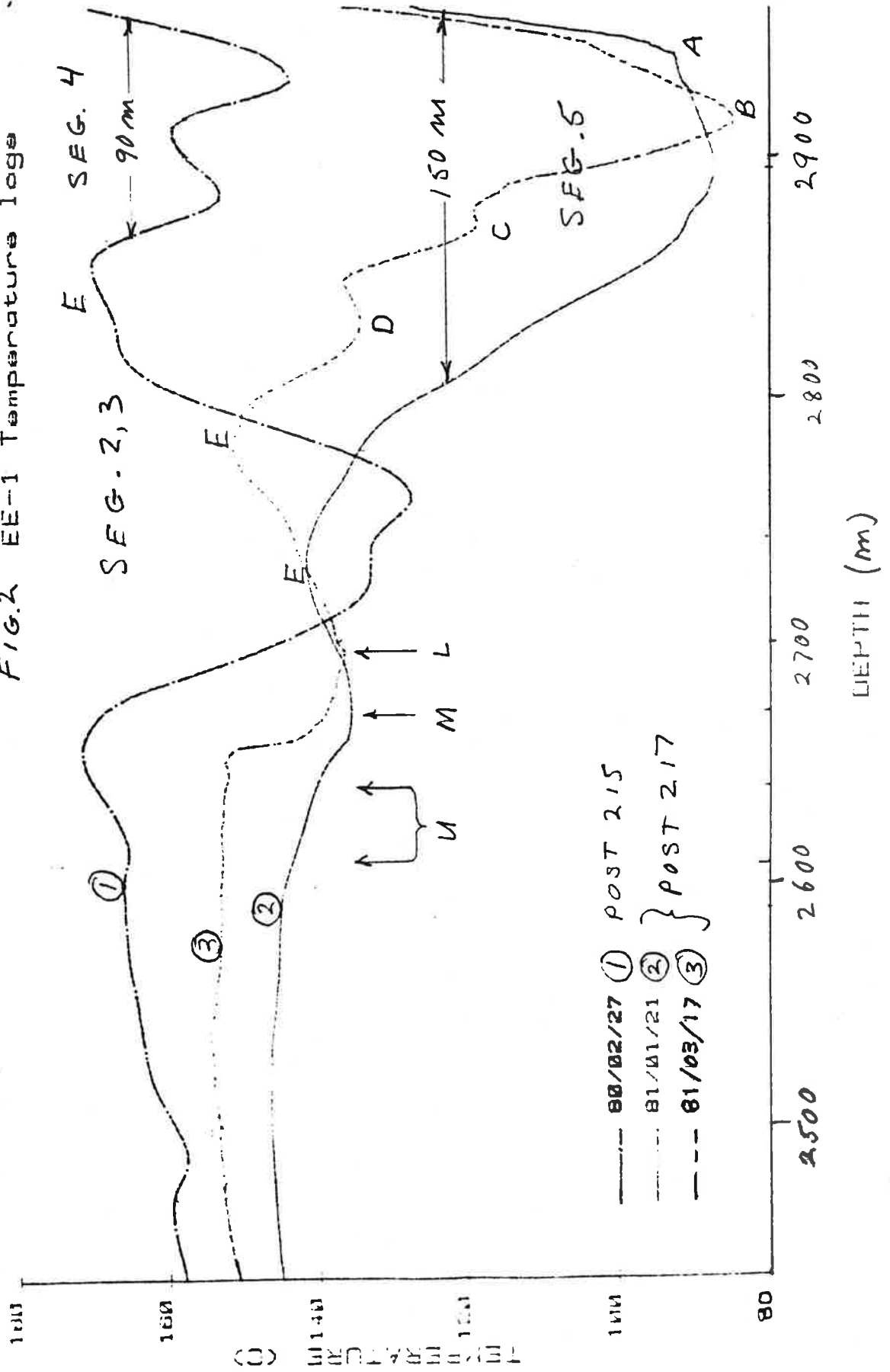


FIG. 2 EE-1 Temperature logs



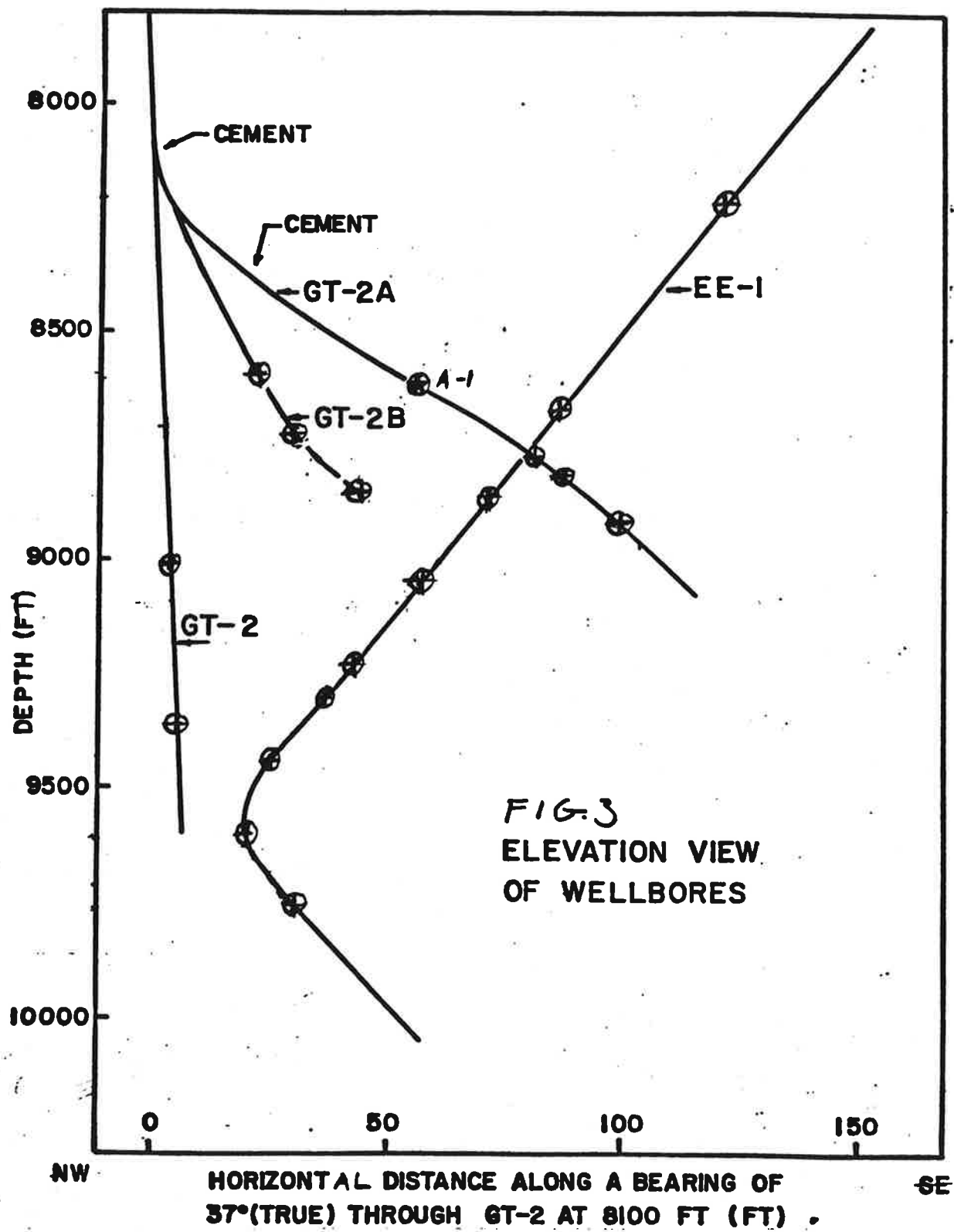


FIG. 3  
ELEVATION VIEW  
OF WELLBORES

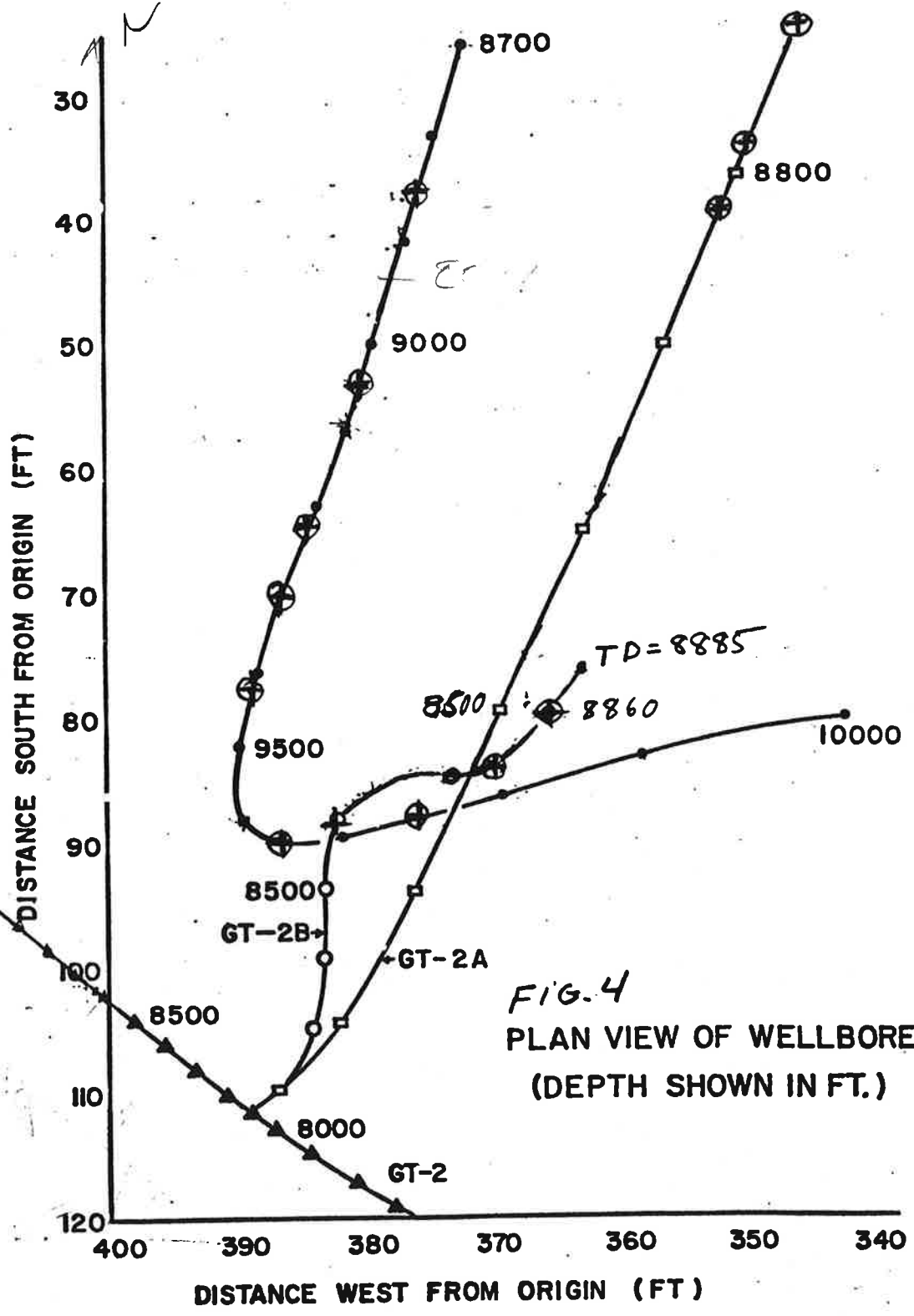
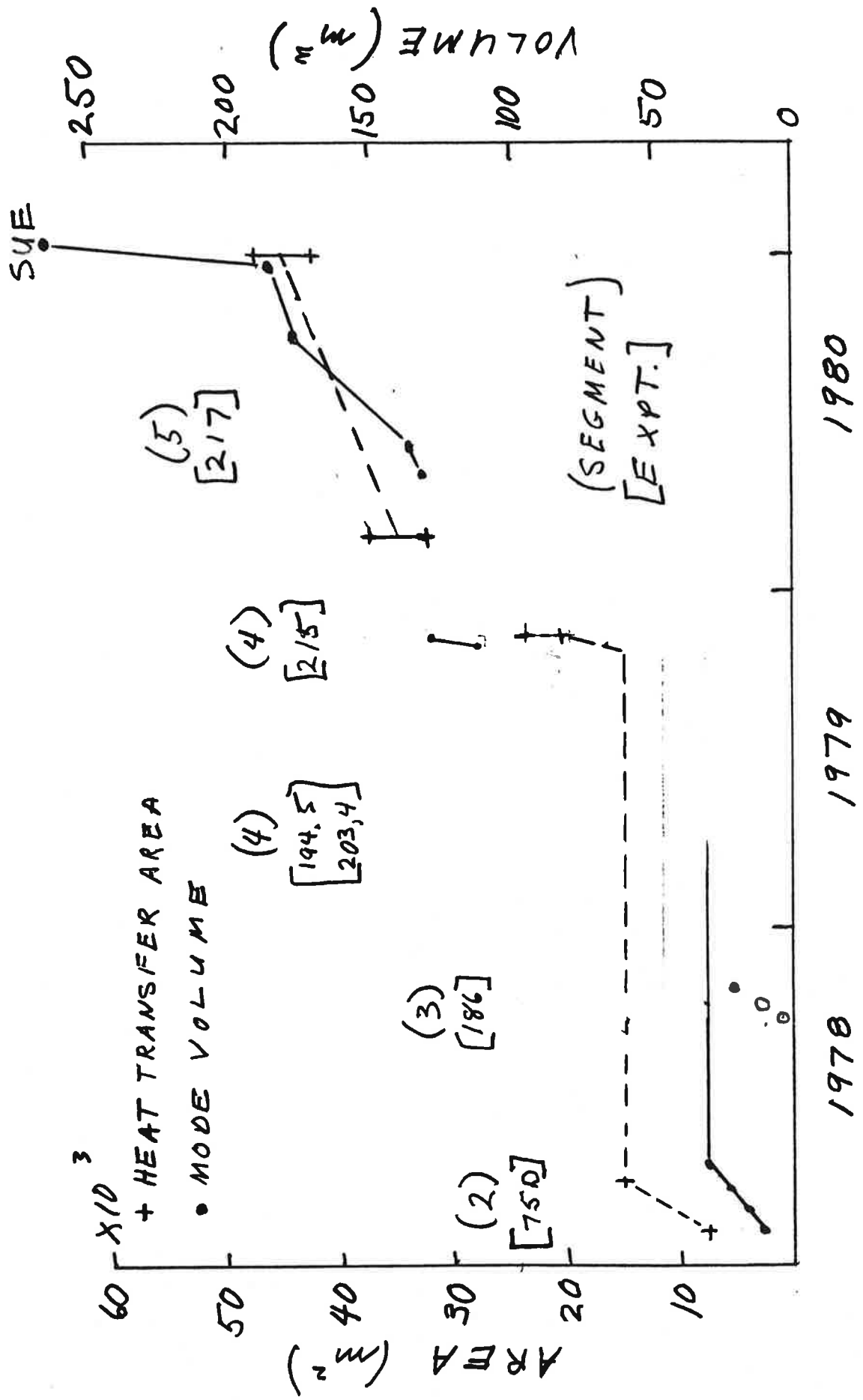


FIG. 4  
 PLAN VIEW OF WELLBORES  
 (DEPTH SHOWN IN FT.)

FIG. 5 PHASE I RESERVOIR: VOLUME AND AREA



APPENDIX C

Water Loss For Expt. 217, H. N. Fisher, January 20, 1981.



OFFICE MEMORANDUM

TO : Distribution

DATE: January 20, 1981

FROM : H. N. Fisher

SUBJECT : WATER LOSS FOR EXP. 217

SYMBOL : G-6

MAIL STOP: 981

I. INTRODUCTION

The water loss data for Segment 5 (experiment 217) have been compared with that of the Segment 2 (75 day test, ref. 1) and Segment 3 (experiment 186, ref. 2). Direct comparisons of the raw data indicate that the water loss rates for the 217 system are approximately 40 percent higher than those of Segment 2. Since the operating pressure (EE-1 surface pressure) was 10 percent higher during Segment 5, the reservoir parameters governing water loss were not more than 30 percent greater for Segment 5 as compared to Segment 2.

Use of the pressure dependent diffusion model (refs. 1, 2, and 3) confirms this comparison. Curve fitting to the water loss rate data with this model also indicates that the reservoir parameters that determine the response to short-term pressure transients is different than that of the Segment 2 reservoir (ref. 3). These short-term transients reflect local properties of the reservoir and indicate that flow in the lower part of the reservoir is governed by a higher stress than the upper (Segment 2)

reservoir. A detailed analysis of the step flow data for experiments 195-204, 215, and 217 is needed to characterize the development of pressure response of this reservoir.

## II. REVIEW OF DATA

Figures 1, 2, and 3 are the raw data for the full duration of Segment 5. Figure 1 is the water loss rate as measured by the make-up pump flow. Figure 2 is the integral of the water loss and Fig. 3 surface pressures. The EE-1 annulus leak which began after day 150 of Segment 5 (labeled (3) in Fig. 1) obscures the water loss data during the last 130 days of the experiment. The seven-day shut-in at day 74 also introduces additional transients at the re-start. The early time data ((1) in Fig. 1) for the first 70 days is best suited to size the system.

The water loss flow rate for Segment 2 is displayed in Fig. 4. The data contains many operational transients and is smoothed by a fit to the pressure-dependent flow model (ref. 1). The break in the data at (1) in Fig. 4 is due to the start of a slow pressure decline in EE-1. The extremely low values of flow at the end of the experiment are due to this transient (ref. 1) and should not be used for comparisons with the Segment 5 system. The early time data is best suited for comparison with other systems.

Water loss measurements were also made during the high back pressure experiment (Exp. 186, of Segment 3, ref. 2) with both EE-1 and GT-2 pressurized. The loss rates of that experiment were equal to or greater than that of Segment 2. The exact amount depends on how much is allotted to the annulus leak at early times. Reference 2 should be consulted for details.

A direct comparison of Figs. 1 and 4 show that for the first 30 days, the flow rates of Segment 5 are somewhat higher than Segment 2. Because of the existence of so many transients, however, the easiest comparison is on the accumulative or integrated losses which smoothed out the transients. The integrated losses are shown in Fig. 5. The dashed curve (2) is Segment 2 scaled linearly to the Segment 5 pressure. The remaining difference is only 30 percent of the Segment 2 losses.

### III. COMPARISON WITH DIFFUSION MODEL

The diffusion model and the resulting fits to the Segment 2 data (the dashed curve of Fig. 4) are detailed in refs. 1 and 3; and, for Segment 3 in ref. 2. The best fit obtained thus far to the Segment 5 data is shown in Fig. 6. The flow transient located at (1) is induced by the pressure steps located at (1) in Fig. 3.

These fits are most sensitive to two parameters: (a)  $\alpha = A\sqrt{k\beta}$  evaluated at starting or hydrostatic pressure. Here A is the diffusing area, k the permeability, and  $\beta$  the system compressibility. (b) C a constant that determines the pressure dependence of  $\alpha$  (see ref. 3). This parameter is best interpreted as the reciprocal of the sum of the confining stress and a fracture modulus.

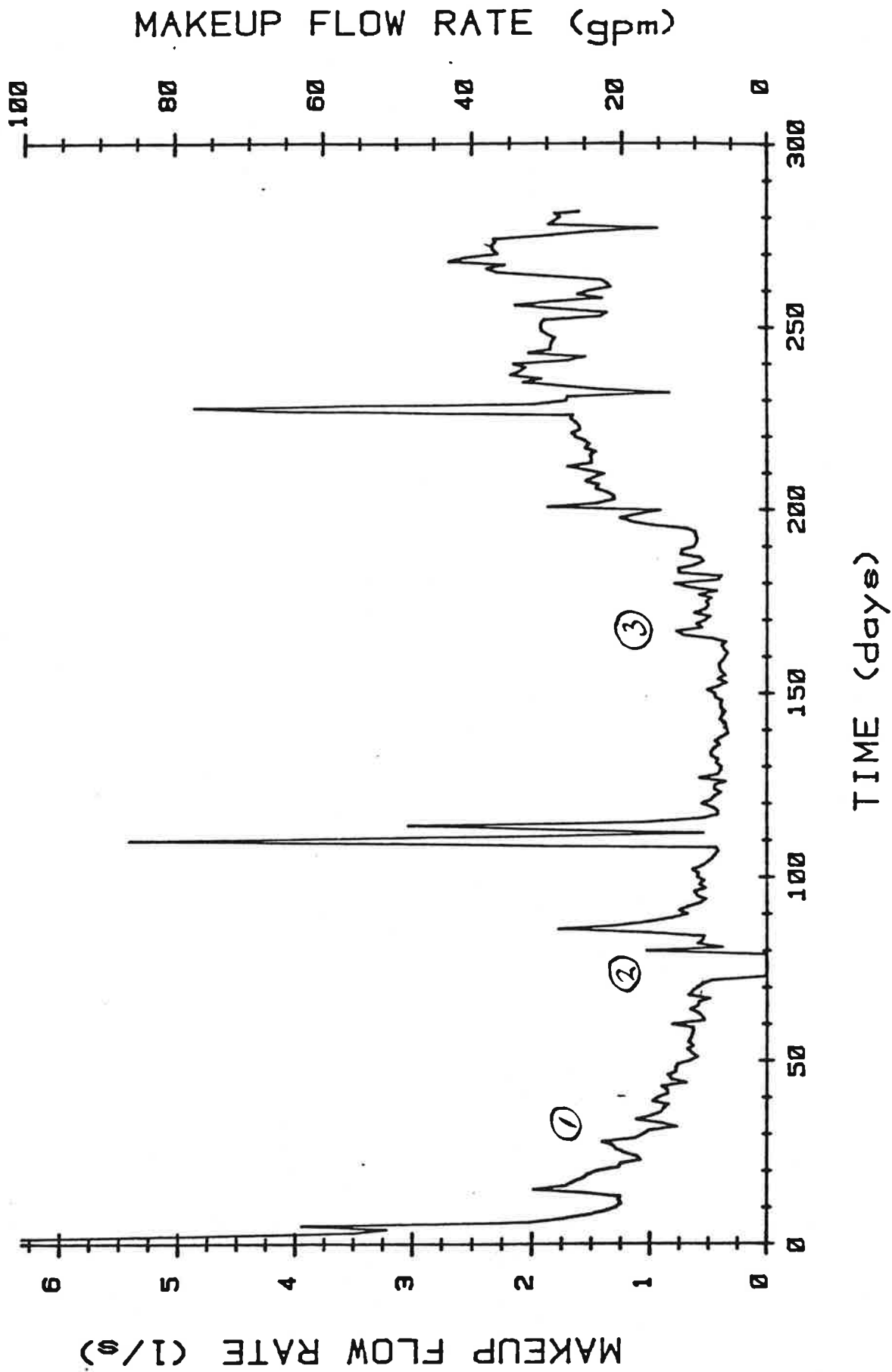
---

NOTE: In all previous reports  $\alpha$  has been reported as the one-sided or one-half the measured value. Also  $\beta$  in  $\alpha$  has been normalized to a rock compressibility of  $2.7 \times 10^{-5} \text{ MPa}^{-1}$ . Here both of these conventions have been discarded and  $\alpha$  is reported as the full measured value in SI units.

---

The current best values for  $\alpha$  at hydrostatic pressure and  $C^{-1}$  obtained from the fits are summarized in the table below.

FIG.1 WATER LOSS RATE ; SEGMENT 5.



Segment	$\alpha (\text{m}^3/\text{MPa}^{-1/2})$	$C^{-1} (\text{MPa})^{-1}$
2	$1.4 \times 10^{-6}$	9.3
3	$1.4 \lesssim \alpha < 2.8 \times 10^{-6}$	9.3
5	$1.9 \times 10^{-6}$	$13.3 \lesssim C^{-1} < 20.0$

The  $\alpha$  for Segment 5 is ~30 percent higher than that of Segment 2 and probably reflects the addition of the lower half of the reservoir. The value of C was determined mainly by one flow transient in segment 5. The range of  $C^{-1}$  indicated in the table reflects the lack of sensitivity to this parameter. Short-term transients, even in the water losses, measure some local parameters. It is possible that the response of lower half of the reservoir is determined by a larger component of in-situ stress.

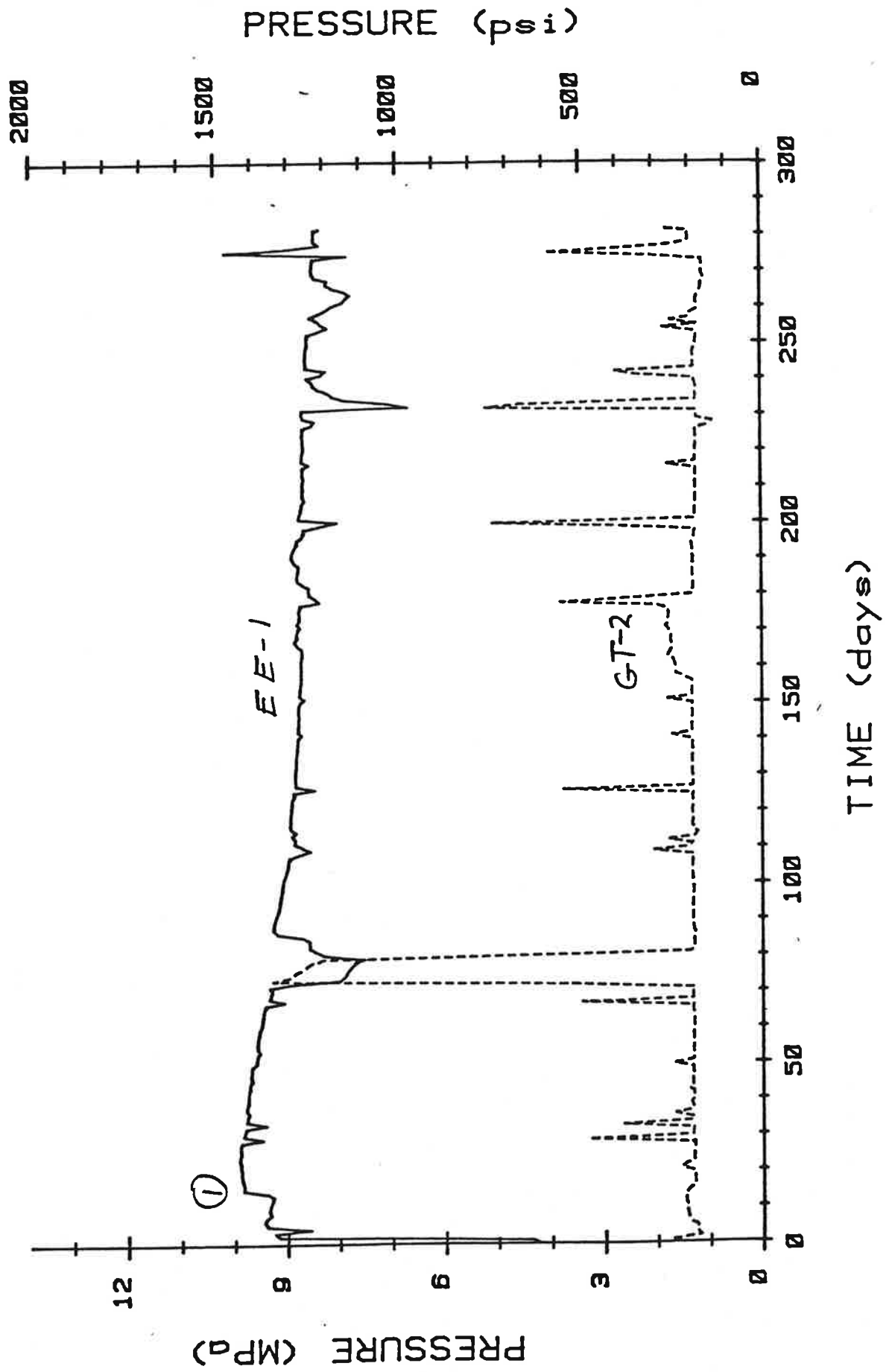
#### REFERENCES

1. J. W. Tester and J. N. Albright (eds.), "Hot Dry Rock Energy Extraction Field Test: 75 Days of Operation of a Prototype Reservoir at Fenton Hill," Los Alamos Scientific Laboratory report LA-7771-MS (April 1979).
2. D. W. Brown, "Results of Expt. 186, The High Back-Pressure Flow Experiment," (in preparation).
3. H. N. Fisher and J. W. Tester, "The Pressure Transient Testing of a Man-Made Fractured Geothermal Reservoir: An Examination of Fracture Versus Matrix Dominated Flow Effect," LA-8535-MS (Sept. 1980).

#### Distribution:

H. Murphy  
 G. Zivoloski  
 Z. Dachs  
 D. Brown  
 C. Grigsby  
 R. W. Spence  
 R. Potter  
 H. N. Fisher  
 G-5 file

FIG. 3 SURFACE PRESSURES



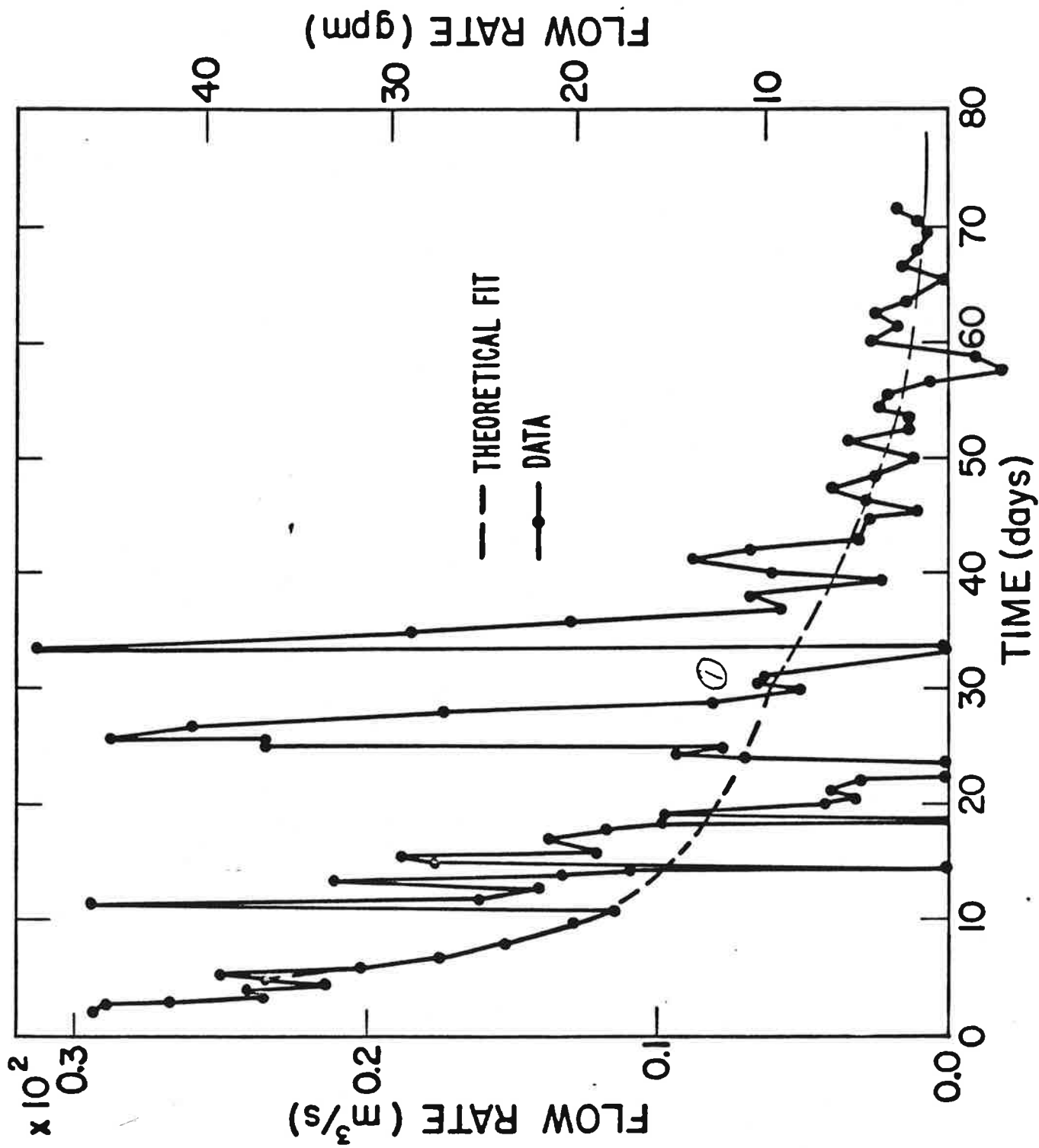


FIG. 4 WATER LOSS RATE DURING SEGMENT 2

FIG. 5 INTEGRATED WATER LOSSES

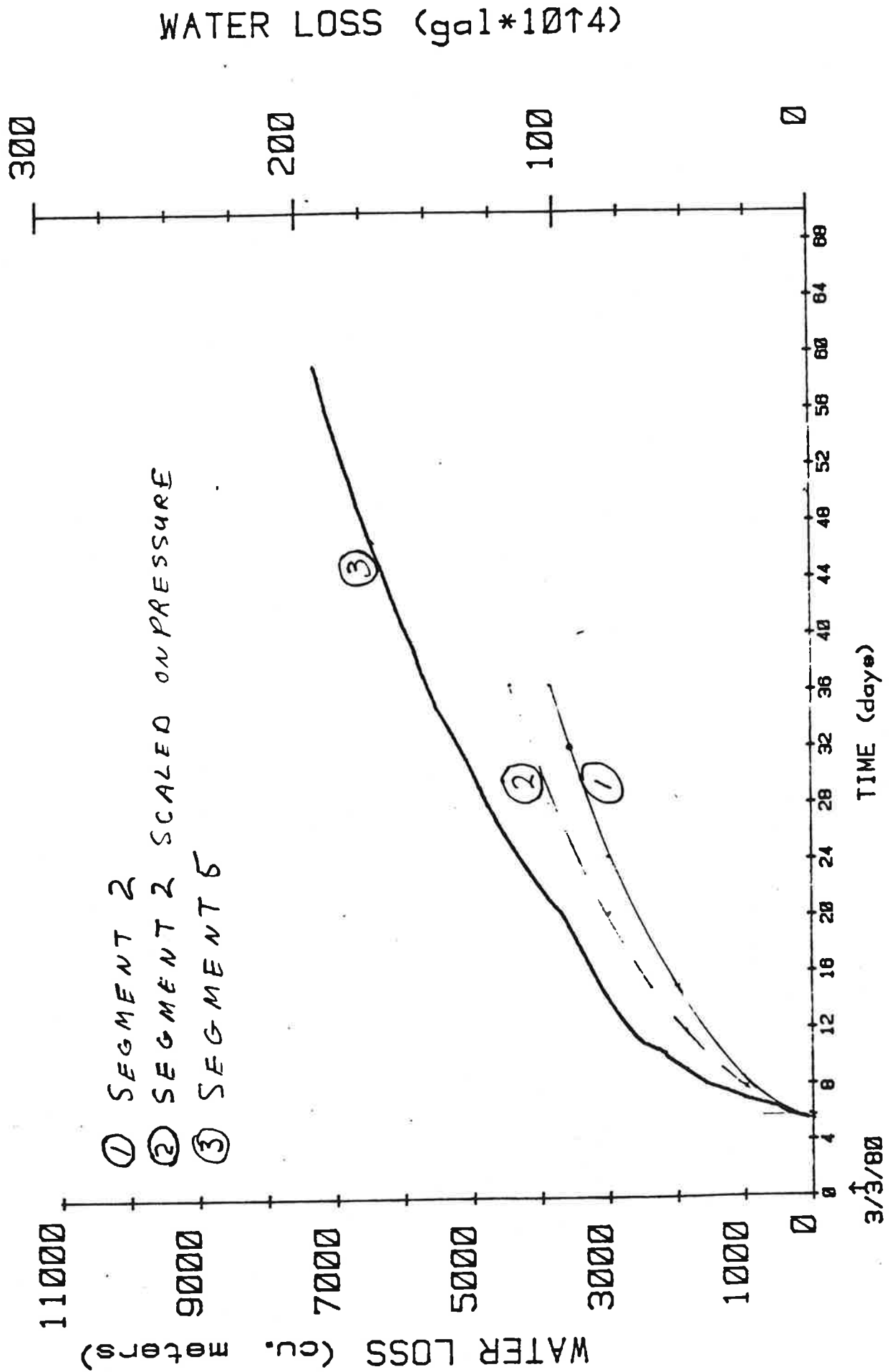
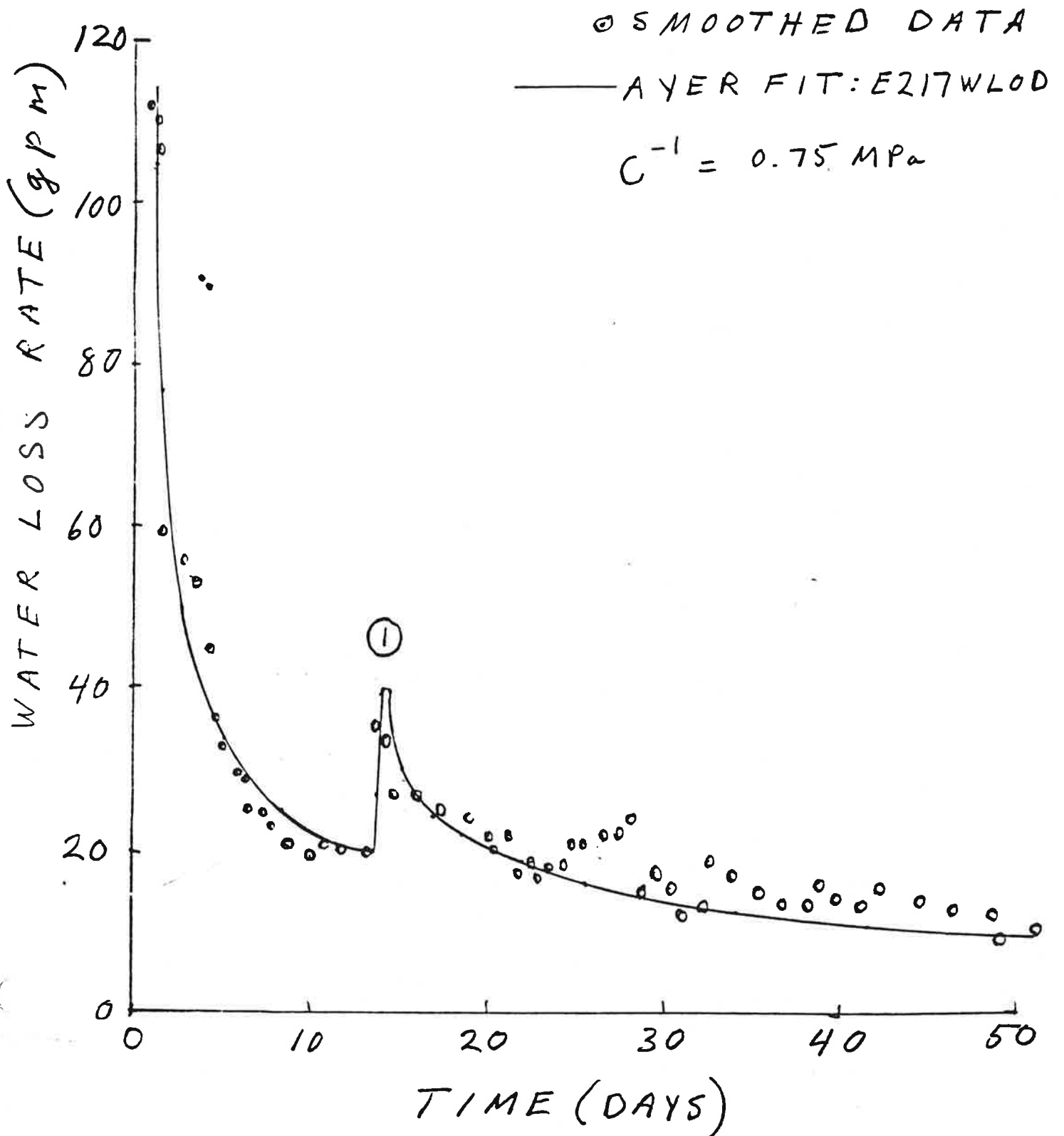


FIG. 6

WATER LOSS RATE:  
EXPT. 217



WATER LOSS (cu. meters)

30000  
25000  
20000  
15000  
10000  
5000  
0

FIG. 2 ACCUMULATIVE WATER LOSS: SEGMENTS

